

The AntAWS dataset: a compilation of Antarctic automatic weather station observations

Yetang Wang^{1*,*}, Xueying Zhang^{1*,*}, Wentao Ning¹, Matthew A. Lazzara², Minghu Ding³, Carleen H. Reijmer⁴, Paul C. J. P. Smeets⁴, Paolo Grigioni⁵, Petra Heil^{6,7}, Elizabeth R. Thomas⁸, David Mikolajczyk², Lee J. Welhouse², Linda M. Keller², Zhaosheng Zhai¹, Yuqi Sun¹, and Shugui Hou^{9*}

¹College of Geography and Environment, Shandong Normal University, Jinan 250014, China

²Antarctic Meteorological Research and Data Center, Space Science and Engineering Center, University of Wisconsin—Madison, Madison, Wisconsin

³State Key Laboratory of Severe Weather, Chinese Academy of Meteorological Sciences, Beijing 100081, China

⁴Institute for Marine and Atmospheric Research Utrecht, Utrecht University, Utrecht, Netherland

⁵Laboratory for Measurements and Observations for Environment and Climate, ENEA, 00123 Rome, Italy

⁶Australian Antarctic Division, Kingston, Tasmania, Australia

⁷Australian Antarctic Program Partnership, University of Tasmania, Hobart, Tasmania, Australia

⁸British Antarctic Survey, Cambridge, UK

⁹School of Oceanography, Shanghai Jiao Tong University, Shanghai, 200240, China

*These authors contributed equally to this work.

*Corresponding to: Yetang Wang (yetangwang@sdu.edu.cn) and Shugui Hou (shuguihou@sjtu.edu.cn)

Abstract. A new meteorological dataset from records of Antarctic automatic weather stations (here called AntAWS dataset) at 3-hourly, daily and monthly resolutions including quality control information is presented here. This dataset integrates the measurements of air temperature, air pressure, relative humidity, and wind speed and direction from 267 AWSs available from 1980 to 2021. The AWS spatial distribution remains heterogeneous, with the majority of instruments located in near-coastal areas, and few inland on the East Antarctic Plateau. Among the 267 AWSs in total, 63 have been operating for more than 20 years, and 27 of them in excess of more than 30 years. Of the five meteorological parameters, the measurements of air temperature have the best continuity and the highest data integrity. The comprehensive compilation of AWS observations has the main aim to make them easily accessible and efficient for use in local, regional and continental studies; it may be accessed at <https://doi.org/10.48567/key7-ch19> (Wang et al., 2022). This dataset is invaluable for improved characterization of the surface climatology across the Antarctic continent, to improve our understanding of Antarctic surface snow-atmosphere interactions, and to evaluate regional climate models or meteorological reanalysis products.

1 Introduction

Against the context of global warming, Antarctica plays an increasing role in the global sea level rise, atmospheric circulation, heat balance and climate evolution, and thus has experienced intense scientific focus (e.g., IPCC, 2019; Kennicutt et al., 2019; Rignot et al., 2019). In recent decades, much attention has been paid to changes to atmospheric variables, such as air temperature, snow accumulation, and wind

37 speed over the Antarctic continent (Huai et al., 2019; Dong et al., 2021; IPCC, 2021), because they have
38 profound impact on the surface energy balance, ice sheet mass changes, as well as the ecosystem in coastal
39 and surrounding regions (e.g., Giovinetto et al., 1990; Gregory et al., 2006; Herbei et al., 2016; Convey
40 et al., 2018). To quantify the underlying variability and trends, accurate and continuous atmospheric
41 measurements are a vital prerequisite.

42 Extensive efforts have been made to obtain continuous atmospheric observations in Antarctica since
43 the International Geophysical Year (IGY) in 1957/1958. For example, a total of approximately 50 staffed
44 stations were established by the end of the IGY, of which 17 have continuous meteorological records to
45 date (Lazzara et al., 2013; Summerhayes et al., 2008). Nevertheless, the majority of the staffed stations
46 are concentrated along the coast, and only seven stations are located in the interior of the Antarctic
47 continent (Allison et al., 1993), which is insufficient to resolve the atmospheric conditions of the interior
48 Antarctica. At the same time, harsh weather conditions and the unique geographical topography of
49 Antarctica make it extremely difficult to install and maintain staffed weather stations. Automatic weather
50 stations (AWSs) has the advantage of gathering meteorological data in remote areas or severe weather
51 conditions, and help to fill the gaps of staffed weather observations (Stearns et al., 1988; Allison et al.,
52 1993; Stearns et al., 1993; Reijmer et al., 2002; Renfrew et al., 2002). A sustained AWS network is
53 required to observe weather and climate across the Antarctic continent (Lazzara et al., 2013).

54 Remote AWS became practical with the introduction of the Advanced Research and Global
55 Observation Satellite network (ARGOS) data relay system on polar orbiting satellites in 1978, and thus
56 real-time or near real-time meteorological data could be obtained from remote places. Based on this,
57 numerous countries independently developed AWSs to support atmospheric observations, glaciological
58 studies, and monitoring projects in Antarctica. In 1979, the United States Antarctic Program (USAP)
59 supported the University of Wisconsin-Madison (UW-Madison) in the deployment of AWSs in Antarctica,
60 mainly located in the Ross Ice Shelf and the West Antarctic Ice Sheet, beyond an initial landmark research
61 effort by Stanford University (Stearns et al., 1993; Lazzara et al., 2012). In 1982, the Australian Antarctic
62 Division (AAD) deployed its first AWS in Antarctica from Casey Station (Allison and Morrissy, 1983).
63 During the International Antarctic Glaciology Program, a network from Casey Station was deployed
64 (Allison et al., 1993). Later, the Australian National Antarctic Research Expedition (ANARE) set up an
65 AWS network with an updated AWS version around the Lambert Glacier (Allison et al., 1998). In 1985,
66 the Italian National Programme of Antarctic Research (PNRA) installed its first AWS, in Terra Nova Bay,
67 named by “Mario Zucchelli”. Currently its AWS network is mainly located in the Victoria Land and
68 Antarctic Plateau. Over the Antarctic Peninsula and Dronning Maud Land, the British Antarctic Survey
69 (BAS, who did collaborate with UW-Madison initially) and the Institute for Marine and Atmospheric
70 Research, Utrecht University (IMAU) installed their respective AWS network. The Chinese National
71 Antarctic Research Expedition (CHINARE) installed their PANDA AWS network, including eleven
72 AWSs from the coast to the summit of the East Antarctic Plateau (Ding et al., 2022). There are other
73 AWS networks in the Antarctic by the different countries (e.g., Japan, France, New Zealand, South Korea).
74 Despite the different designs of AWSs between nations, it is common that all stations measure air
75 temperature, air pressure, relative humidity, and wind speed and direction.

76 Given the funding constraints of different national Antarctic programs, AWSs provide the most
77 economical way to gather weather data to support ongoing applications, field activities and the planning
78 of maintenance visits. Early scientific studies based on AWSs focused on the local meteorological

79 processes and climatology of some basic parameters, such as temperature, pressure and wind (Stearns et
80 al.,1993; Allison et al.,1993; Aristidi et al., 2005; Seefeldt et al., 2007). Over the Antarctic Ice Sheet (AIS),
81 there are still missing data values at each AWS, which are a constraint for the climatological studies.
82 Spatial and temporal interpolations are often used to fill the data gaps, and as a result, some continuous
83 time series of meteorological elements have been created (e.g., Shuman and Stearns, 2001; Bromwich et
84 al., 2013, 2014; Reusch and Alley, 2004). In addition, the AWS observations have also been used to
85 evaluate and validate reanalysis products, regional climate models and remote sensing retrievals (e.g.,
86 Gallée et al., 2010; Tastula et al., 2012; Wang et al., 2013; Huai et al., 2019). Antarctic AWS observations
87 are also used in the glaciological studies, such as estimation of snow accumulations (e.g., Wang et al.,
88 2021), calculation of the surface energy balance (e.g., van Wessem et al., 2014), and understanding the
89 AIS mass changes (e.g., Knuth et al., 2010).

90 To better characterize the regional or even continental weather and climate status over Antarctica, many
91 attempts have been made to compile all available past and present AWS observations into the Antarctic
92 climate database. Jacka et al. (1984) carried out the pioneering work to compile all annually and monthly
93 averaged temperature observations of Antarctic and Southern Ocean island stations. Jones et al. (1987)
94 assembled an integrated annual and monthly mean sea level pressure and temperature dataset from 29
95 weather stations located at 60°S-90°S. Stearns et al. (1993) provided a detailed description of the monthly
96 mean climate data including monthly mean and extreme values of temperature, pressure, wind speed and
97 direction collected and processed by the Antarctic AWSs at UW-Madison. The dataset is being
98 continuously updated. Turner et al. (2004) described the Reference Antarctic Data for Environmental
99 Research (READER) by the Scientific Committee on Antarctic Research (SCAR). The dataset includes
100 the monthly and annual mean near-surface air temperature, pressure and wind speed data from 43 staffed
101 stations and 61 AWSs. Rodrigo et al. (2013) compiled Antarctic surface wind observations from 115
102 AWSs to assess the performance of regional climate models, and ERA-40 and ERA-Interim reanalysis
103 products. These AWS observation compilations generally suffer from part or all of the following
104 limitations: the duration of datasets, single meteorological parameter, low temporal resolution, limited
105 spatial coverage, limited or no rigorous quality control, and in some cases limited availability for the
106 public. Most recently, Kittel compiled a near-surface weather observation database at a high temporal
107 resolution, which to a great extent remedied the deficiency of the previous database (Kittel, 2021), and
108 has already been used in the studies of the ice sheet surface processes, climate model validation and
109 atmospheric diagnoses (e.g., Donat-Magnin et al., 2020; Mottram et al., 2021; Kittel et al., 2021; Kittel,
110 2021; Wille et al., 2021). However, these data were only qualitatively compared with models to detect
111 and remove any outliers, and they are still not available for the public. Thus, better composition and
112 quality control could allow for a more reliable dataset.

113 In this study, our main goal is to use all available records from AWSs to construct a comprehensive
114 quality-controlled database of Antarctic meteorological parameters including air temperature, pressure,
115 relative humidity, and wind speed and direction. The database is 3-hourly, daily, and monthly resolved.
116 We describe the methods used to generate this dataset, including record inclusion criteria and data quality
117 control. In addition, the main temporal and spatial features of the database are summarized.

119 AWSs are ground-based meteorological data collection devices, which can run without any support all
120 year round. All Antarctic AWSs are similar in design. They are equipped with a set of standard
121 independent sensors, following the standards of the World Meteorological Organization (WMO, 2018).
122 The UW-Madison AWS network at the Antarctic Meteorological Research Center (AMRC) initially
123 consisted of dataloggers developed in-house at UW-Madison, with the AWS 2B series becoming their
124 primary electronics system in the 1980s and early 1990s. Beginning in the late 1990s, UW-Madison
125 switched to using commercial off-the-shelf dataloggers manufactured by Campbell Scientific. Currently,
126 the primary AWS system used by the AMRC is consists of a Campbell Scientific CR1000 device
127 datalogger, which is a commercial off-the-shelf system wired and programmed much like AMRC's
128 original AWS 2B series. The CR1000 datalogger has the ability of keeping track of additional weather
129 observations on AWSs that the AWS 2B system does not such as snow accumulation and
130 incoming/outgoing shortwave/longwave radiation. Initially, AWSs employed by the BAS used
131 collaborated with UW-Madison, and then switched to use the CR1000 datalogger for measurements. The
132 IMAU Antarctic AWS Project also uses the CR1000 device and a homemade system. Most of the AWSs
133 of the PNRA are acquisition and control units provided by Vaisala series. The glaciology program of the
134 AAD has designed and built three different types of AWSs during the past 20 years, with the latest version
135 being series 098 AWSs. The CHINARE AWSs consist of standard components provided by Campbell
136 and Vaisala series, except the XFY3-1 sensor (domestic propeller anemometer) (Ding et al., 2022). The
137 supporting framework for AWS instruments varies between models, but in general, the AWS body is
138 made up of a mast and instrument arms fitted with different sensors. The AWS datalogger, satellite
139 transmitter, pressure sensor, power regulating circuit and battery are generally installed in a box (or a
140 series of boxes) at the bottom of the mast. In summer, the battery is charged by a small solar panel installed
141 vertically near the top of the mast. However, the sensors of the AMRC AWS are mounted on Rohn tower
142 sections, and similar towers have been used by others. Table 1 presents the different types of sensors used
143 on the AWSs and the corresponding detailed techniques. Although the instrument manufacturers may
144 vary across the different AWS networks, the measuring range, accuracy and resolution are identical or
145 nearly similar. Figure 1 shows the typical AWSs in four Antarctic research projects, but other AWS may
146 have different sensors depending on the local environment.

147 An AWS system can store meteorological observational data onto a datalogger, which is convenient
148 for managing operations (e.g., DT50, CR1000, etc.). The datalogger transmits the observations through
149 the ARGOS, carried by the National Oceanic and Atmospheric Administration (NOAA) (NOAA-19 and
150 earlier) and Metop series of polar orbiting satellites. Figure 2 shows the data acquisition diagram of the
151 AWSs, taking the Wisconsin AMRC AWS relay network as an example. One of the ways that AMRC
152 receives the ARGOS' data (the archive data) is directly through file transfer protocol (FTP) services from
153 Service ARGOS complete worldwide collection system, including all data (e.g., repeated data
154 transmissions, etc.). These data are regularly processed into meteorological values via the quality control,
155 and then provided to the community. AMRC also has a set of AWS units using the Iridium
156 communications system much like this.

157 Each AWS measures air temperature, pressure, relative humidity and other meteorological elements
158 within a height range of ~1 to 6 m, which are the initial height when the AWS was installed without

159 including the snow accumulation changes and site tilt, except for Zhongshan Station, which measures
 160 wind speed and wind direction at a height of 10 m. In fact, due to the accumulation of snow, the
 161 measurement height of each meteorological element varies over time, which may result in the notable
 162 meteorological observation disparities such as temperature and wind speed caused by the instrument
 163 height differences. Some AWS also measure air temperature, wind speed and other variables at different
 164 heights to provide near ground vertical gradient data, which is convenient to check the accuracy of data
 165 and the redundancy of certain sensors. Some AWSs have added sensors that measure snow temperature
 166 at different depths, solar radiation and snow depth, as well as a series of internal management parameters,
 167 such as voltage and internal temperature (see Fig.1).

168 Cost-effective AWSs provide timely research data from remote areas of Antarctica throughout the year.
 169 Maintenance is still needed, and generally one visit is performed per summer to ensure that electric power
 170 generation and battery capacity are sufficient for polar night operation. However, several AWSs are not
 171 revisited after initial deployment. For example, since its first deployment in October 1984, AWS GC41
 172 has been operating continuously in the interior of Antarctica with no maintenance access. The accuracy
 173 of the data from these sites can only be estimated by the internal consistency of the diverse sensors.
 174

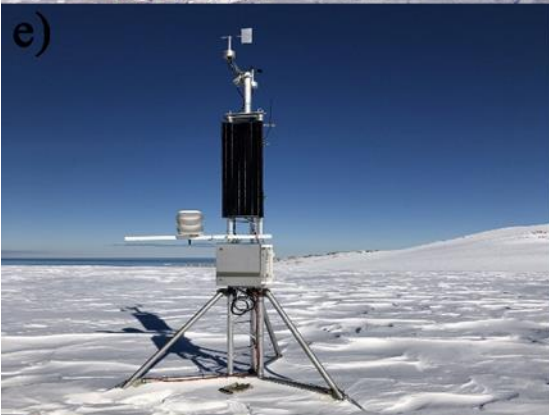
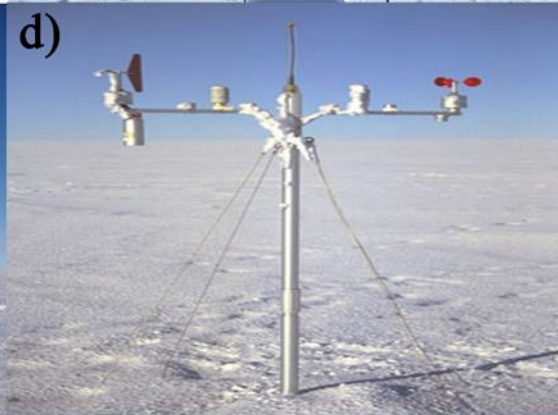
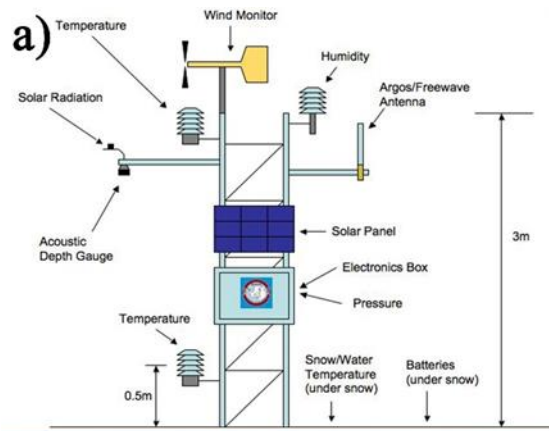
175 Table 1. The sensor types used on the automatic weather stations and the technical specifications.

Institution	Sensor	Type	Specifications		
			Range	Resolution	Accuracy
AMRC	Air temperature	Weed PRT Two-wire bridge	to -100°C minimum	0.125°C	±0.5°C
		RM Young 43347 RTD 1000-ohm PRT	to -100°C minimum	0.01°C	±0.3°C
		Apogee ST-110 Thermistor	to -100°C minimum	0.01°C	0.1°C above 0°C 0.15°C below 0°C
	Relative humidity	Vaisala HMP14UT	0 to 100%	0.04%	±4%
		Vaisala HMP31UT Vaisala HMP35A/D Vaisala HMP45A/D	0 to 100%	0.04%	±2% above -20°C
		Vaisala HMP155	0 to 100%	0.04%	±2% above -40°C ±5% above -40° to -60°C
	Air pressure	Paroscientific Model 215 A	0 to 1100 hPa	0.04 hPa	±0.1 hPa
		CSI 105/PTB101	0 to 1100 hPa	0.1 hPa	±3 hPa
		CSI 106/PTB110	500 to 1100 hPa	0.1 hPa	±1.5hPa
	Wind speed	Bendix Model 120 Aerovane	0 to 60 m s ⁻¹	0.25 m s ⁻¹	±0.5 m s ⁻¹

		Belfort Model 122/123			
		RM Young 05103/106	0 to 60 m s ⁻¹	0.2 m s ⁻¹	±0.3 m s ⁻¹
		Taylor Model 201 High Wind System	0 to 60 m s ⁻¹	0.33 m s ⁻¹	±2 m s ⁻¹
	Wind direction	Bendix Model 120 Aerovane Belfort Model 122/123 RM Young 05103/106/ Taylor Model 201 High Wind System	0 to 360°	1.5°	±3°
PNRA	Air temperature	Vaisala HMP45C/D	-40 to +60°C	-	±0.2°C
		Vaisala HMP155	to -80°C minimum	-	(0.2260-0028*Ta) °C
	Relative humidity	Vaisala HMP45D	0 to 100%	0.04%	±2% above -20°C
		Vaisala HMP155	0 to 100%	0.04%	±2% above -40°C ±5% above -40° to -60°C
	Air pressure	CS106 Barometer	500 to 1100 hPa	0.1 hPa	±1.5 hPa (-40 to +60°C)
		BARO1	500 to 1100 hPa	0.01 hPa	±0.15 hPa (-40 to +60°C)
		PTB200	600 to 1100 hPa	0.01 hPa	±0.15 hPa (-40 to +60°C)
	Wind speed	Vaisala WAA151	0.4 to 75 m s ⁻¹	-	±0.5 m s ⁻¹
		RM Young 05103/106	0 to 60 m s ⁻¹	0.2 m s ⁻¹	±0.3 m s ⁻¹
	Wind direction	Vaisala WAV151	0 to 360°	2.8°	±3°
RM Young 05103		0 to 360°	1.5°	±3°	
IMAU	Air temperature	Vaisala HMP35AC	-80 to +56°C	-	±0.3°C
	Relative humidity	Vaisala HMP35AC	0 to 100%	-	±2% (RH<90%) ±3% (RH>90%)
	Air pressure	Vaisala PTB101B	600 to 1060 hPa	-	±4 hPa
	Wind speed	RM Young 05103	0 to 60 m s ⁻¹	0.2 m s ⁻¹	±0.3 m s ⁻¹
	Wind direction	RM Young 05103	0 to 360°	1.5°	±3°
AAD	Air temperature	FS23D thermistor in ratiometric circuit	-99 to +13°C	0.02°C	±0.05°C
	Relative humidity	Vaisala HMP35D	0 to 100%	2%	±2% (RH<90%) ±3% (RH>90%)
	Air pressure	Paroscientific Digiquartz 6015A	0 to 1100 hPa;	0.1 hPa	±0.2 hPa

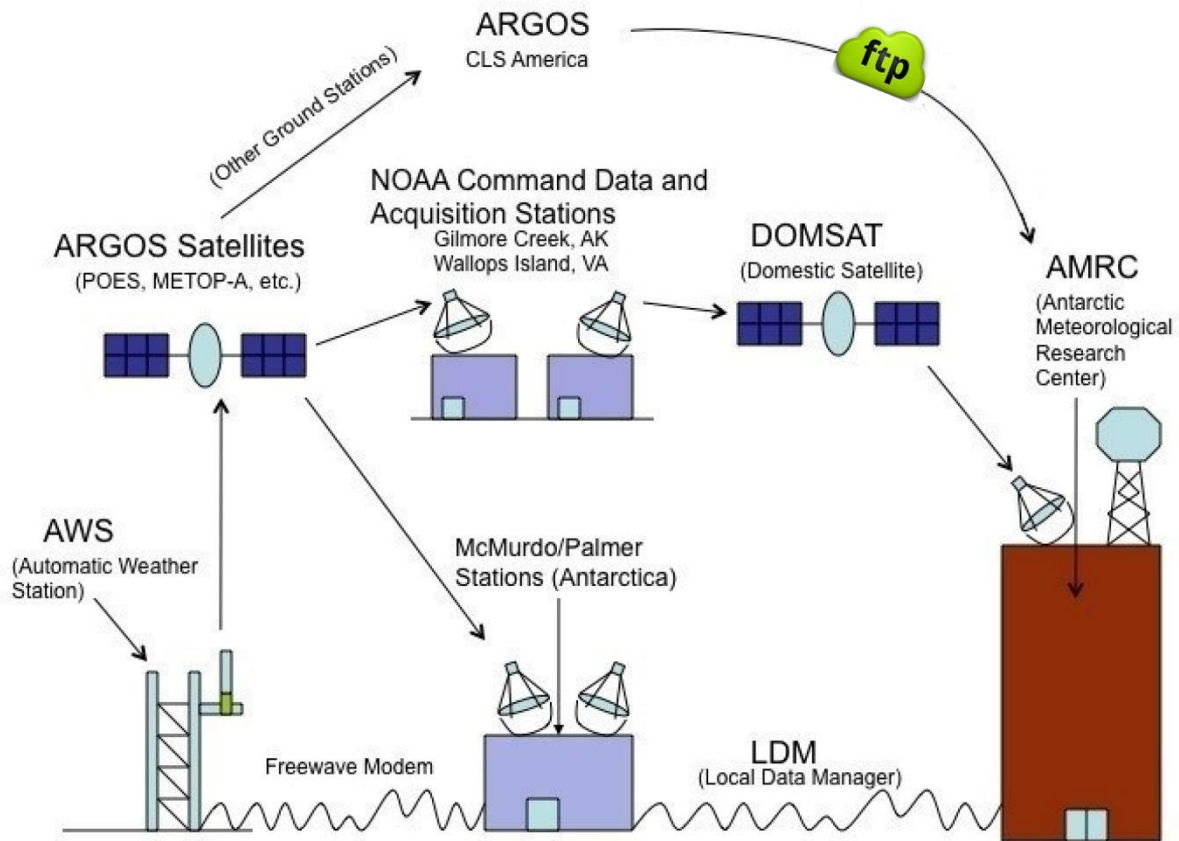
			DomeA: 530 to 610 hPa; Eagle: 635 to 735 hPa; LGB69: 691 to 791 hPa		
	Wind speed	3-cup anemometer with R M Young 12170C cup set, and AAD built body and mechanism	0 to 51 m s ⁻¹	0.1 m s ⁻¹	±0.5 m s ⁻¹
	Wind direction	Aanderaa 3590B wind vane Aanderaa 2750	0 to 360°	6°	±6°
BAS	Air temperature	CSI RTD 100-ohm PRT	to -100°C minimum	0.01°C	±0.5°C
		Weed PRT Two-wire bridge	to -100°C minimum	0.125°C	±0.5°C
		Vaisala HMP35D/45D	-40 to +60°C	-	±0.2°C
	Relative humidity	Vaisala HMP35D	0 to 100%	2%	±2% (RH<90%) ±3% (RH>90%)
		Vaisala HMP45A/D	0 to 100%	0.04%	±2% above -20°C
	Air pressure	Paroscientific Model 215 A	0 to 1100 hPa	0.04 hPa	±0.1 hPa
	Wind speed	Propeller-vane anemometer	-	-	-
		Belfort Model 122/123	0 to 60 m s ⁻¹	0.25 m s ⁻¹	±0.5 m s ⁻¹
		RM Young 05103/106	0 to 60 m s ⁻¹	0.2 m s ⁻¹	±0.3 m s ⁻¹
Wind direction	Propeller-vane anemometer	-	-	-	
	Belfort Model 122/123 RM Young 05103/106	0 to 360°	1.5°	±3°	
CHINARE	Air temperature	HMP155 resistance probe	to -80°C minimum	-	(0.2260-0028*Ta) °C
		Campbell 109	-	-	(0.2260-0028*Ta) °C
		FS23D thermistors	-99 to +13°C	0.02°C	±0.05°C
		Weed PRT Two-wire bridge	to -100°C minimum	0.125°C	±0.5°C
	Relative humidity	HMP155	0 to 100%	0.04%	±2% above -40°C ±5% above -40° to -60°C

		HMP35A/D	0 to 100%	0.04%	±2% above -20°C
	Air pressure	CS106 Barometer	500 to 1100 hPa	0.1 hPa	±1.5 hPa (-40 to +60°C)
		PTB110	0 to 1100 hPa	0.1 hPa	±1.5hPa
		PTB210	-	-	±0.5hPa
		6015A	0 to 1100 hPa; DomeA: 530 to 610 hPa; Eagle: 635 to 735 hPa	0.1 hPa	±0.2 hPa
		Paroscientific Model 215 A	0 to 1100 hPa	0.04 hPa	±0.1 hPa
	Wind speed	XFY3-1	0.3 to 50 m s ⁻¹	-	±1m s ⁻¹
		12170C	0 to 51 m s ⁻¹	0.1 m s ⁻¹	±0.5 m s ⁻¹
		RMYoung	0 to 60 m s ⁻¹	0.2 m s ⁻¹	±0.5 m s ⁻¹
	Wind direction	XFY3-1	0 to 360°	-	±5°
		10K Ohmpot	0 to 355°	1.5°	±3°
		3590B	0 to 360°	6°	±6°
POLENET	Air temperature	Vaisala WXT520	-	-	±3°C
	Relative humidity	Vaisala WXT520	-	-	±3%
	Air pressure	Vaisala WXT520	-	-	±3 hPa
	Wind speed	-	-	-	-
	Wind direction	-	-	-	-



178 Fig.1. Typical AWSs of the six research institutions, but the sensors at other sites vary slightly
 179 depending on the local environment. a) AMRC-CR1000 device, b) AMRC- AGO-4, c) AMRC and
 180 CHINARE-Panda_South, d) IMAU-AWS10, e) PNRA-Maria, f) AAD-LGB00, g) BAS-the sensors
 181 used on Latady, h) BAS-Latady.

- 182 a) <http://amrc.ssec.wisc.edu/news/2010-May-01.html>
 183 b) https://amrc.ssec.wisc.edu/aws/images/station_images/AGO_4.jpg
 184 c) personal communication with Minghu Ding.
 185 d) <https://www.projects.science.uu.nl/iceclimate/aws/technical.php>
 186 e) <https://www.climantartide.it/attivita/aws/index.php?lang=en>
 187 f) personal communication with Ian Allison
 188 g) and h) <https://ramadda.data.bas.ac.uk/repository/entry/show?entryid=synth%3A44d1a477-0852-4620-a1f4-63f559b44e94%3AL0RvY3VtZW50cy9waG90b3NfYXZz>
 189
 190



191 Fig.2. Data acquisition diagram of AWS, using AMRC as an example.
 192 http://amrc.ssec.wisc.edu/aws/images/datastream_v2.jpg
 193

194 **3 Data processing**

195 **3.1 Data collections and sources**

196 The AWS meteorological observations were obtained from seven Antarctic AWS project databases,
197 including the CHINARE (<https://doi.org/10.11888/Atmos.tpdc.272721>), the BAS
198 (<https://data.bas.ac.uk/datasets.php>), the PNRA (<http://www.climantartide.it>), the IMAU Antarctic AWS
199 Project (<https://www.projects.science.uu.nl/iceclimate/aws/antarctica.php>) (data available from
200 <https://doi.org/10.1594/PANGAEA.910473>), the AAD (<http://aws.cdaso.cloud.edu.au/datapage.html>),
201 the AMRC (<http://amrc.ssec.wisc.edu/>) at the University of Wisconsin (Lazzara et al., 2012), and the
202 Polar Earth Observing Network (POLENET) program (<https://www.unavco.org/>). The AMRC includes
203 not only its own AWS network but also brings together data from several Antarctic research programs,
204 such as the Japanese Antarctic Research Expedition (JARE), the French Antarctic Program (Institut
205 Polaire Francais-Paul Emile Victor, IPEV), the AAD, the BAS and the CHINARE. The JARE installed
206 and maintained JASE2007, Dome Fuji, Mizuho and Relay Station on the East Antarctic Plateau. The
207 IPEV installed and took charge of the AWSs from the Adélie Coast to Dome C, including Port Martin,
208 D-10, D-17, D-47, D-85, Dome C and Dome C II. Cape Denison AWS on the Adélie Coast is serviced
209 by the AAD. The BAS installed and maintained the AWSs on the Antarctic Peninsula and the East
210 Antarctic Plateau, including Butler Island, Larsen Ice Shelf, Limbert, Sky-Blu, Fossil Bluff, Dismal Island
211 and Baldrick. The PANDA-South AWS, located on the East Antarctic Plateau, is a cooperation between
212 CHINARE and AMRC, which was installed, maintained and operated by CHINARE.

213 First, we excluded AWS with data coverage of less than one year. Then, all available records from the
214 remaining stations were collected. Finally, measurements from 267 AWSs were compiled, including at
215 least one of the five meteorological variables: near surface air temperature, relative humidity, air pressure,
216 wind speed and wind direction. Fig.3 shows the spatial distribution of the 267 AWSs, and the
217 corresponding longitude and latitude coordinates, elevation and data sources of these AWSs are
218 summarized in Table S1.

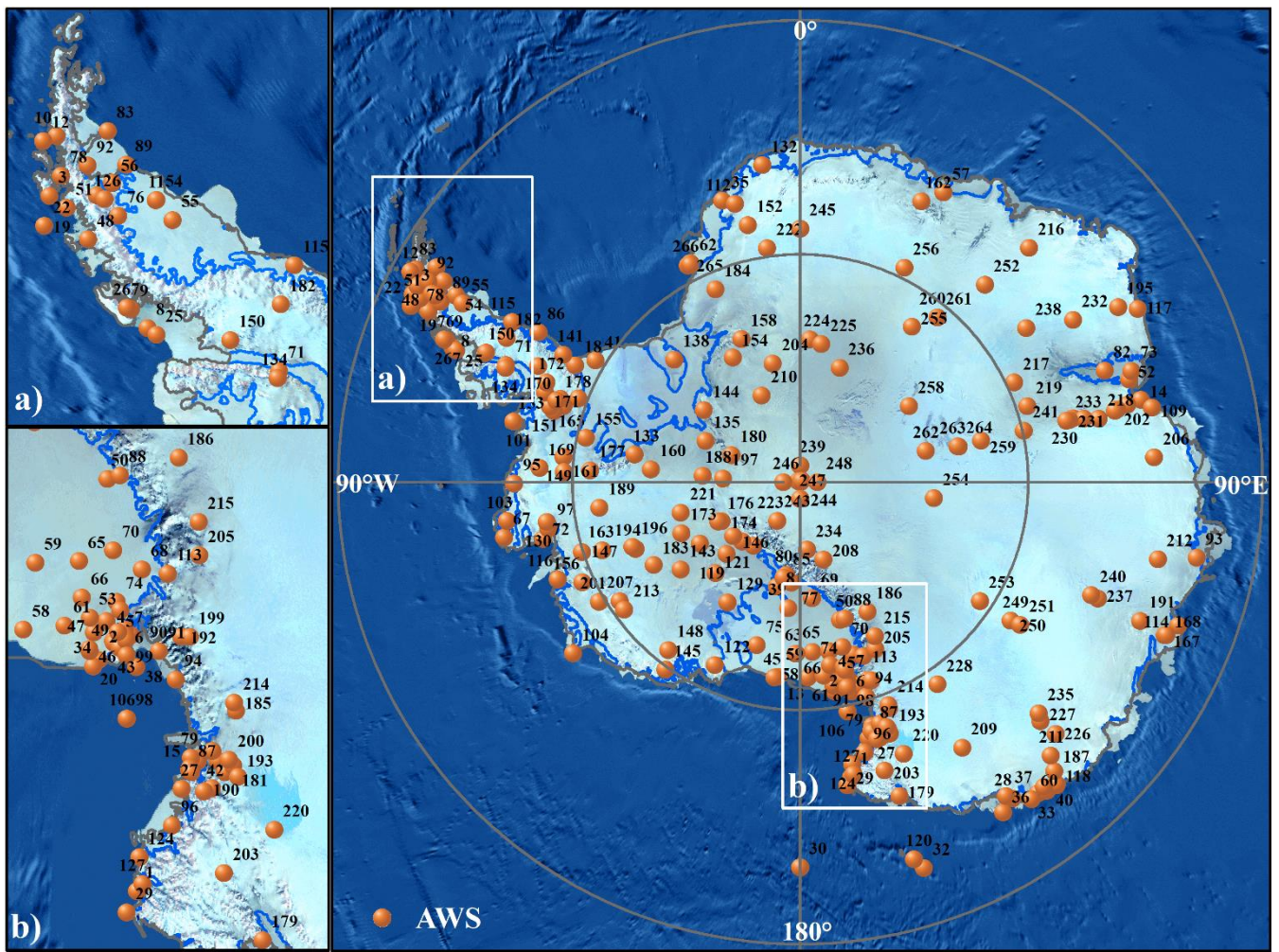
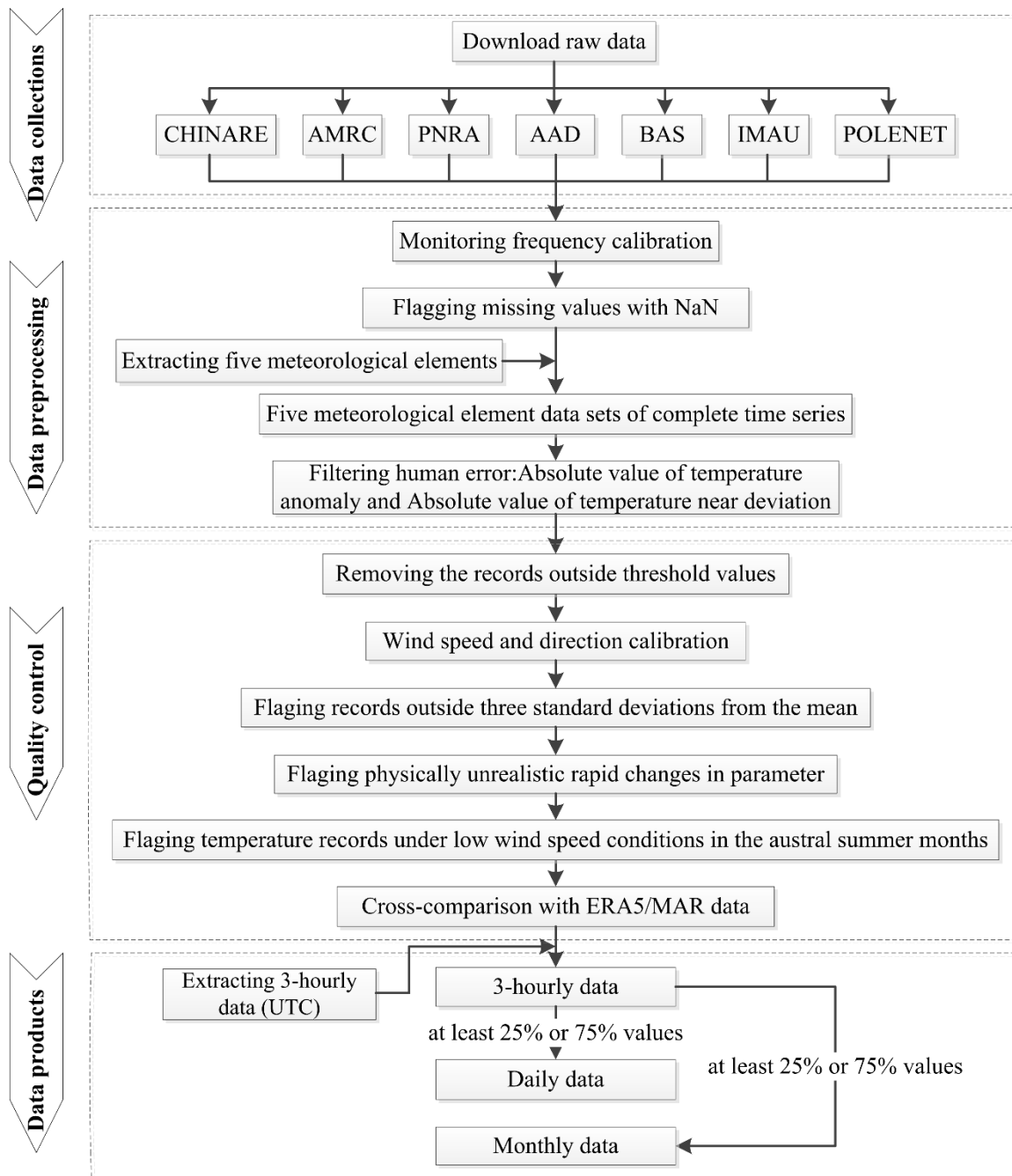


Fig.3. Map of the 267 Automatic Weather Stations (AWS) in this study, where the numbers (1-267) correspond to NO. in Table S1.

219
220
221
222

223
224



225
226 Fig.4. Description of AWSs data processing process.

227 **3.2 Quality control**

228 The quality check of observational data is aimed at detecting missing data and errors to provide the highest
229 possible standard of accuracy. Our compilation is based on the hourly and 3-hourly synoptic

230 measurements from AWSs, which were subjected to quality checks by data providers, including: a coarse
 231 error check using threshold values at the time of decoding; manually filtering errors or gaps due to the
 232 presence of instrument failures such as sensor freezing and screen covered by snow/frost; transmissions
 233 issues through the datalogger, Global Telecommunications System (GTS) or ARGOS; and changes in
 234 units. Despite the quality checks, previous studies pointed out that cautions should be made on using these
 235 AWS data, at least wind speed data, which are the least reliable variable of the measurements (e.g., Stearns
 236 et al.,1993). To perform a more rigorous quality control, a set of interactive quality control programs
 237 using interactive data language (IDL) software was developed for the quality check of the AMRC data
 238 (Lazzara et al., 2012). In our compilation, we use the 3-hourly AMRC AWS data through preliminary
 239 quality control. Since our objective was to construct a dataset with high quality, restrictive quality control
 240 criteria were used to filter the compiled data from a variety of sources.

241 First, we removed the records from the dataset outside the measurement range of sensors installed over
 242 the AWSs (Table 2). Data with zero values for both wind speed and direction were also eliminated.
 243 Furthermore, if the wind speed and direction values remained unchanged for 6 consecutive hours which
 244 are likely caused by sensor freezing, the values were set to the null values (NA). Secondly, the mean and
 245 standard deviation were calculated for the 3-hourly data in each month. We also checked physically
 246 unrealistic rapid synoptic variability in the parameters using the 6-h change threshold values of 10 hPa
 247 for surface pressure, 5°C for air temperature, 40 kt for wind speed (Turner et al., 2004). Following Lazzara
 248 et al. (2012), the observation values exceeding three standard deviations from the mean were considered
 249 to be possibly erroneous, and thus were flagged. Thirdly, we flagged the air temperature records in the
 250 austral summer months (December-January-February) during the low-wind speed conditions (less than
 251 2 m s^{-1}), which can result in a warm temperature bias during this period because of the lack of ventilation
 252 (Genthon et al., 2011; Lazzara et al., 2012; Jones et al., 2016). At last, after these physically-based filters,
 253 we performed a visual cross-comparison of each time series of the filtered data with the corresponding
 254 outputs of ERA-5 (Hersbach et al., 2020) and MAR (Kittel, 2021), to
 255 further remove outliers and improve the reliability of the dataset.

256
 257 Table 2. Threshold values used in the quality control process for each measured variable.

Variable	Units	Low threshold	High threshold
Temperature	°C	-100	15
Pressure	hPa	0	1100
Wind Speed	m/s	0	60
Wind Direction	°	0	360
Relative Humidity	%	0	100

258 3.3 Averaging procedure

259 For all meteorological parameters, daily and monthly mean values are calculated by the 3-hourly data
 260 (eight values a day, between 00:00 and 21:00 UTC). Unfortunately, a number of occurred events may
 261 result in data gaps because of only checked periodically. For daily values to be included, at least two 3-
 262 hourly observed values (25%) must be available in that day, since less than 25% of the 3-hourly
 263 observations do not well capture the weather conditions of a day, and a good daily average cannot be

264 obtained. Then, if at least 25% of the 3-hourly observations are available in a month, we calculate a
265 monthly average. For monthly data, when less than 25% of the 3-hourly observations are available, this
266 value typically occurs when a station starts or stops during the month. This may lead to the deviation of
267 the monthly average, especially in the period of rapid changes in meteorological elements such as air
268 temperature. All missing values are set to NA. To provide more reliable daily and monthly values, we
269 also calculate the daily and monthly products using a 75% threshold, that is, at least six 3-hourly observed
270 values are available, as in Kittel (2021).

271 **4 Description of the AntAWS dataset**

272 **4.1 Air temperature**

273 Air temperature is a sensitive indicator of the climate extremes experienced by the whole continent. It is
274 measured at the heights of approximately 3 m above the ground, using a thermistor (such as Apogee ST-
275 110 Thermistor and FS23D thermistor in ratiometric circuit) or resistive platinum probe (such as PRT
276 series and Vaisala HMP series). The air temperature sensor is installed in the AWS' naturally ventilated
277 radiation shields to protect the sensor from direct sunlight, and the measurement uncertainty is within
278 $\pm 0.5^{\circ}\text{C}$. It should be emphasized that over areas with strong temperature inversions, especially the
279 Antarctic Plateau in winter, near-surface air temperature is influenced by changes in the height of sensors
280 installed on the AWS (generally a relative "lowering") caused by snow accumulation (Genthon et al.,
281 2021).

282 Figure.5 and Table S2, Table S3, Table S4 show the mean, maximum and minimum values of 3-hourly,
283 daily, and monthly air temperature from each AWS. The overall statistical results show the effects of sea-
284 land distribution and elevation, as the air temperature in coastal areas is generally higher than that in
285 inland areas, showing a gradual decrease from coastal to inland areas. The near-surface temperature is
286 evidently affected by elevation and decreases significantly with the elevation increase (Fig.5). Fig.6 and
287 Table S2 show that the mean temperature of 3-hourly data ranges from -59.94°C to 2.13°C . The extreme
288 maximum temperatures of the Antarctic Peninsula, most of the West AIS, Ross Ice Shelf and Victoria
289 Land are almost all over 0°C . The warmest AWSs are South Georgia 1, South Georgia 3 and King Edward
290 Pt, with the elevations of 85 m, 53 m and 346 m respectively, and the maximum temperature can reach
291 15°C . The AWSs with extreme minimum temperatures below -70°C are mainly distributed in the East
292 Antarctic Plateau. The minimum temperature value is lower than -82°C , occurring at aws12, aws13,
293 Dome C and Dome F. Statistics of the daily air temperature indicate that the daily mean air temperature
294 values range from -58.42°C to 2.36°C (Table S3). The maximum daily temperature occurs at King
295 Edward Pt station on the Berkner Island, reaching 13.95°C . The lowest daily temperature is -83.51°C at
296 aws13. According to the statistical results of monthly data in Table S4, the mean temperature of monthly
297 data ranges from -59.02°C to 2.32°C . The King Edward Pt station still has the highest monthly averaged
298 air temperature of 5.9°C . Concordia, located on the East Antarctic Plateau, has the lowest monthly
299 temperature of -71.76°C .

300 **4.2 Air pressure**

301 All the AAD AWSs use Paroscientific digiquartz barometers, with an accuracy of ± 0.2 hPa and a
302 resolution of 0.1 hPa. AMRC AWSs also use Paroscientific digiquartz barometers (Paroscientific Model
303 215 A), which have a higher resolution of 0.04 hPa and accuracy of ± 0.1 hPa. Most AWSs at other
304 institutions use Vaisala's PTB series and Campbell's CS series. Both series of barometers use Vaisala's
305 BAROCAP silicon capacitive absolute pressure sensor, which have excellent accuracy, repeatability, and
306 long-term stability over a wide range of operating temperatures. The barometer, kept in the electronics
307 enclosure measures, the station pressure and is not corrected to sea level. The accuracy of all air pressure
308 measurements ranges from 0.15 hPa to 4 hPa, depending on the sensor used.

309 Fig.6 and Table S2 show the mean, maximum and minimum pressure of the 267 AWSs at 3-hourly
310 time resolution. The range of the mean air pressure values goes between 573.49 hPa and 996.24 hPa.
311 AWSs with 3-hourly average pressure greater than 900 hPa are mainly located along the coast of the Ross
312 Ice Shelf, Antarctic Peninsula, Dronning Maud Land, the Lambert Glacier Basin, and Victoria Land. The
313 maximum 3-hourly air pressure is 1039.2 hPa at South Georgia 3, followed by the station on the Larsen
314 Ice Shelf of the Antarctic Peninsula. The minimum (536 hPa) is present at Dome A station, with an
315 elevation of 4093 m. Mainly affected by elevation, the mean, maximum and minimum air pressure
316 decreases with the increase of altitude and spatially decreases from the coast to the interior (Fig. 5). The
317 major features of the spatial distribution of daily and monthly air pressure are almost the same as those
318 of 3-hourly data.

319 **4.3 Relative humidity**

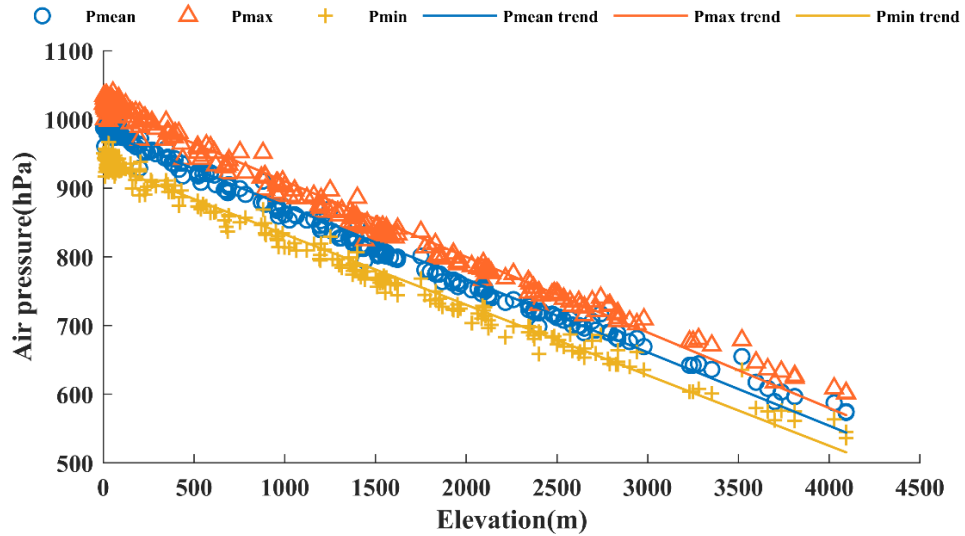
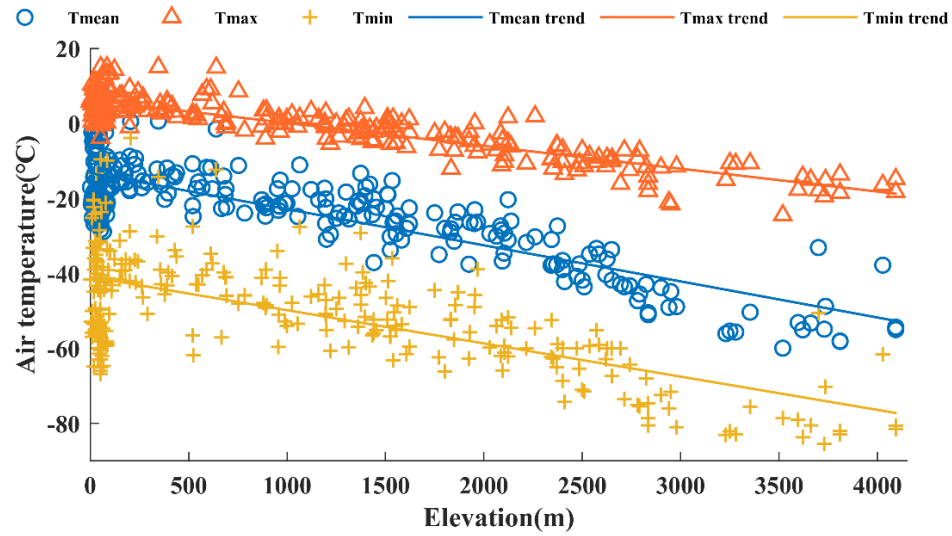
320 The height of the humidity sensor is often the same as that of the air temperature probe. Correct
321 measurements of relative humidity are key to calculate sublimation. However, it is quite difficult to
322 accurately measure, especially in Antarctica. The original network did not include such measurements,
323 but humidity detectors (Vaisala HMP Series) have been deployed since about 1990. Humidity
324 measurements are based on a capacitive thin film polymer sensor. The resolution of the series of humidity
325 sensors is approximately 1%, and the annual drift in the field is approximately $\pm 2 \sim 3\%$. The Vaisala
326 humicap, which itself takes the conversion of ice and water form into account, is factory calibrated to
327 provide RH with respect to liquid water even at below-freezing temperatures (Amory, 2020; Genthon, et
328 al., 2013). The relative humidity is computed with respect to liquid water. Data should be converted to
329 get RH with respect to ice using the method of Goff and Gratch (1945) (Amory, 2020), but these additional
330 computed data are left for forthcoming papers. In Antarctica, even near the surface, the relative humidity
331 with respect to ice often reaches well over 100%, and this is especially frequent on the high Antarctic
332 plateau where supersaturation often occurs (Genthon et al., 2017, 2022). The sensors used on the AWS
333 cannot report supersaturation and measure humidity above 100%, and as a consequence the humidity data
334 are biased low there.

335 Many AWSs lack relative humidity measurements in consecutive years or entirely, which brings great
336 challenges to humidity research over the whole Antarctic continent. The relative humidity of the coastal
337 AWSs is usually higher than that of the inland AWSs, and shows similar spatial patterns with air
338 temperature.

339 4.4 Wind speeds and directions

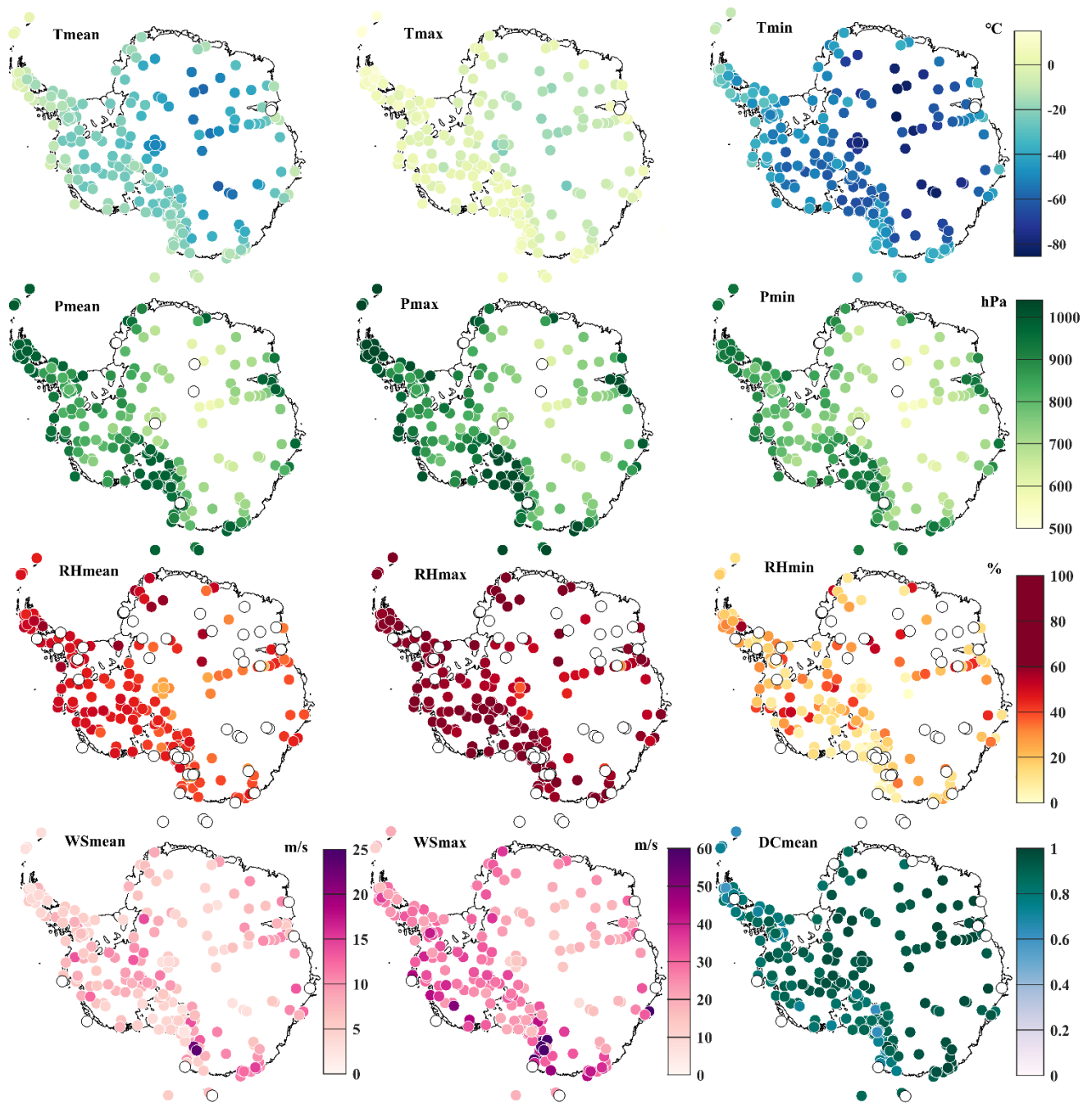
340 Wind speeds and directions are monitored at a height of approximately 3 m above the ice sheet surface
341 (Lazzara et al., 2012). It is notable that at the Zhongshan station, the 10 m wind directions are measured.
342 Due to the influence of katabatic wind, the wind directions at this station are relatively stable and resemble
343 the 3m wind directions (Ma et al., 2014). Different sensors are used to measure wind speed and direction
344 at different AWSs. The most widely used model is R. M. Young Company 05103/106, in which wind
345 speeds are measured using an impeller anemometer that is a helical, four-blade impeller. The rotation of
346 the impeller generates a signal proportional to wind speeds, and wind directions are measured using a
347 potentiometer. In addition, some AWSs adopt the heated Vaisala WA15 series, which is based on precise
348 sensors mounted on cross arms. Its WAA151 anemometer has the characteristics of fast response and low
349 threshold. Similarly, the optoelectronic vane-WAV151 has the advantages of counterbalance, sensitivity,
350 accuracy and low threshold. It is more suitable for more demanding wind measurements. The
351 measurement accuracy of wind speeds is approximately $\pm 0.5 \text{ m s}^{-1}$, and wind direction is $\pm 3^\circ$. The wind
352 direction listed is clockwise from 0° to 360° (so 90° are east, 180° are south, and 270° are west). The
353 stations established by CHINARE use a domestic propeller anemometer (XFY3-1 sensor), which can
354 measure the wind speed and direction of horizontal airflow at very low critical wind speed, with an
355 uncertainty of $\pm 1 \text{ m s}^{-1}$ and $\pm 5^\circ$, respectively (Ding et al., 2022). It is important to recall that wind speed
356 varies strongly with height in the first few meters above the surface, and the height of the sensors above
357 surface gradually decreases with snow accumulation, causing poorly known variations of the instrument
358 height above the snow surface and affects the data quality and consistency (Genthon et al., 2021). Still,
359 information on the evolution of wind speed with time is important, but the modulus is not well known
360 and not consistent in the dataset. To improve the accuracy of air temperature and wind observations, the
361 vertical temperature and wind profiles should be corrected by accounting for the sensor height variations,
362 as done by Ma et al. (2008) and Smeets et al. (2018). However, this additional computed data will be left
363 until we have sufficient snow height data.

364 The results of Fig.6 and Table S2, 3 and 4 show that wind speed is consistent whether parsed in 3
365 hourly values or in daily and monthly values, and so is wind direction. The mean near-surface wind speeds
366 of the 267 AWSs vary from 2.17 to 23.66 m s^{-1} . The average wind speed is higher along the East AIS
367 coast, where the average wind speed exceeds 20 m s^{-1} (e.g., Cape Denison, Lucia, Virginia and Zoraida
368 stations). The average wind speed at AGO-5, Dome C, Dome F, and Dome A stations on the Antarctic
369 inland plateau is less than 3 m s^{-1} , mainly due to the gentler surface slopes of the inland plateau (Van den
370 Broeke and Van Lipzig, 2003). The maximum wind speed (exceeding 60 m s^{-1}) is observed at Alessandra,
371 Eneide, Lanyon, Lola, Lucia, Minna Bluff, Rita, Silvia, Sofia, Sofiab, Virginia and Zoraida stations in
372 North Victoria Land. Spatial patterns of wind speed are generally high along the coast and low on the
373 inland ice sheet, which is mainly determined by the terrain and pressure gradient from coastal to inland.
374 Southerly or easterly winds prevail over most of the AIS, influenced by circumpolar westerly winds,
375 katabatic winds, large-scale pressure gradient forces and topography, which contributes to drive the
376 movement of the AIS atmospheric boundary layer (Van den Broeke et al., 2002). The winds over the AIS
377 are persistent throughout most of the year, which is reflected in a high mean value of daily mean constancy
378 of the wind direction (defined as the ratio of the magnitude of the mean wind vector to the scalar average
379 wind speed) (≥ 0.6) for the majority of the AWSs (Fig.6).



381
382
383

Fig.5. Multiyear 3-hourly mean, maximum and minimum air temperature and pressure as a function of elevation.



384
385
386
387
388
389

Fig.6. Spatial distribution of AWS' multiyear 3-hourly mean, maximum and minimum meteorological elements (temperature, pressure, relative humidity, wind speed) and daily mean constancy of the wind direction (DC) during 1980-2021. White circles represent missing data. Tmean is mean temperature, Tmax means maximum temperature, Tmin is minimum temperature, Pmean is mean pressure, Pmax is maximum pressure, Pmin is minimum pressure, RHmean is mean relative humidity, RHmax is maximum

390 relative humidity, RHmin is minimum relative humidity, WSmean is mean wind speed, WSmax is
391 maximum wind speed, and DCmean is daily mean constancy of the wind direction.

392 **5 Spatiotemporal characteristics of the AntAWS dataset**

393 **5.1 Spatial coverage of AWS records**

394 The spatial distribution of AWSs is heterogeneous over the AIS. On the whole, since 1980, the number
395 and coverage of AWSs have been gradually increasing (see Fig.7, Fig.8, and Table S5). In 1980, there
396 were only 9 AWSs, of which five were located in the Ross Island Vicinity, two stations on the coast of
397 Adélie Land, and two in inland Antarctica (Byrd and Dome C). The number and spatial coverage of AWSs
398 when their data are available peak in 2014, with a total of 146 AWSs. Approximately 90% of the AWSs
399 were distributed in coastal areas and regions of lower elevation. Among them, the densest regions covered
400 by AWSs are the Ross Ice Shelf and Victoria Land, accounting for approximately 50% of AWSs in 2014.
401 The gradually improved AWS network has helped fill the wide gaps in climate observations across the
402 whole Antarctic continent.

403 Despite the significant improvement of the spatial coverage of AWSs, the data availability are still not
404 regularly distributed and are clustered in specific areas of Antarctica (see Fig.6, Table S5). Air
405 temperature and pressure are relatively easy to measure, have the highest data availability of any sensor,
406 and have high integrity and wide spatial coverage. Additionally, the quality of air temperature data is the
407 best, with only two stations missing air temperature measurement records. Measuring wind speed and
408 direction is a huge challenge in Antarctica, however, due to covering such a wide range of speeds from
409 calm/breeze to sustained hurricane intensity. A more challenge is that wind sensors freezing/breaking due
410 to environmental conditions (snow/riming, high winds, etc.). The loss of wind speed and direction data
411 mainly occur in the coastal areas of the Lambert Glacier Basin, Wilkes Land, Victoria Land, Mary Byrd
412 Land and Ellsworth Land. The humidity sensors may lose measurement accuracy at very cold
413 temperatures, and their data loss is highest. In addition to the West AIS and near the South Pole, there are
414 many AWSs that lack humidity measurements all year round in other parts of Antarctica.

415
416

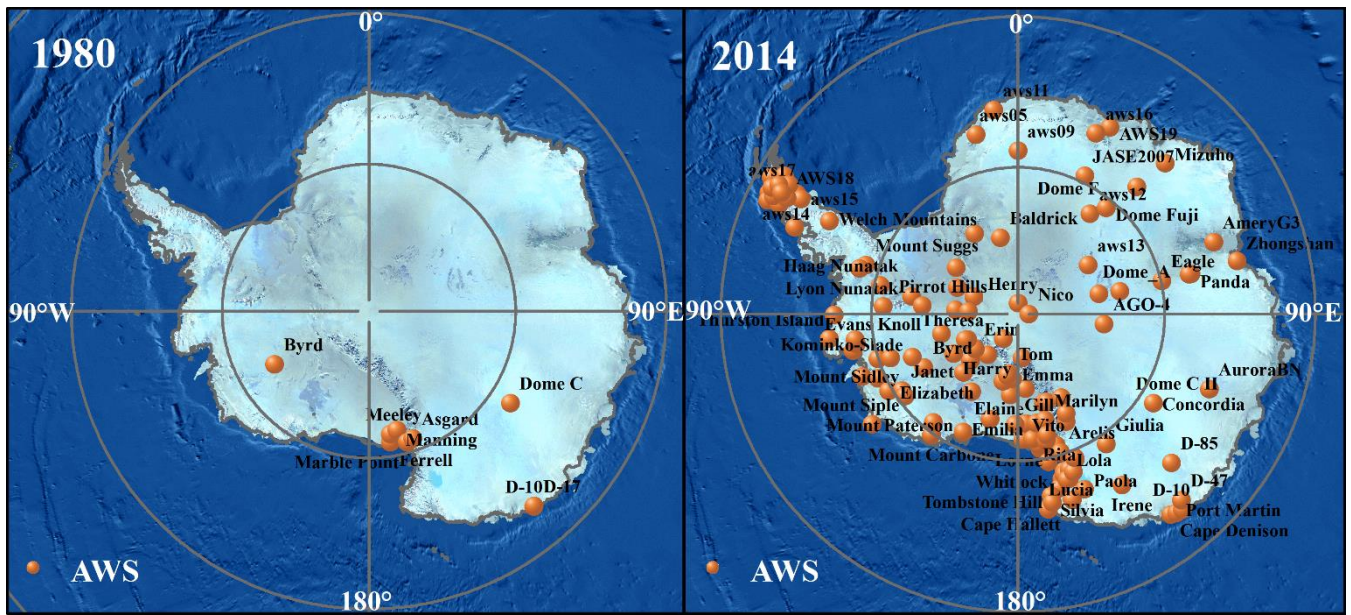


Fig.7. Spatial distribution of AWS in 1980 and 2014

417
418
419
420

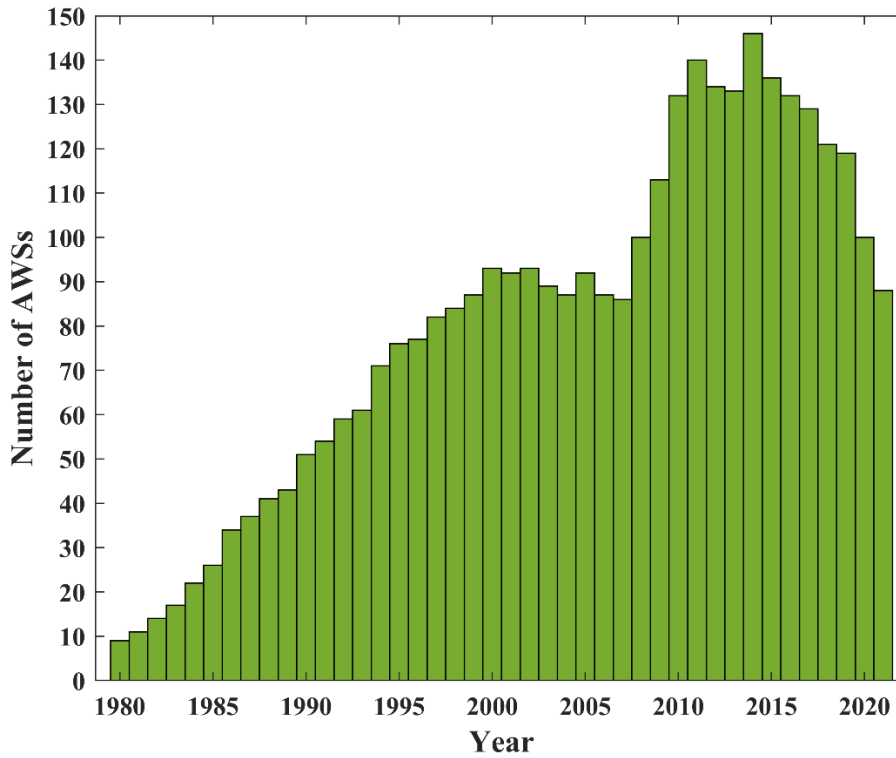


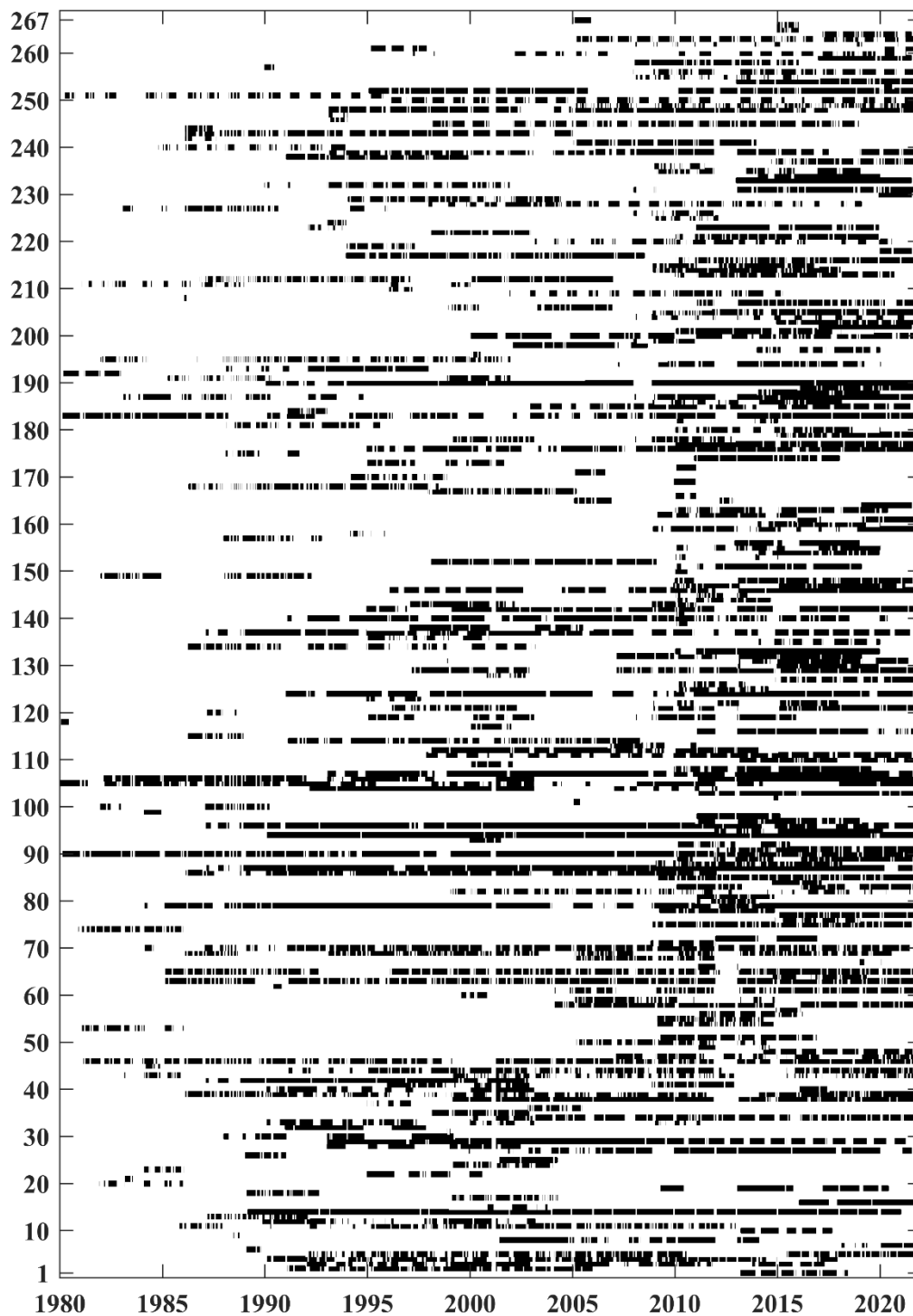
Fig.8. Number of AWSs counted each year.

421
422

423 **5.2 Temporal variability in the AWS records**

424 The five meteorological elements of each AWS cover different time spans, from 1 year to 42 years. The
425 time period covered is closely related to sensor technology and weather conditions. Statistical results in
426 supplemental Table S5 show that the time span of 63 AWSs exceeds 20 years, of which 27 stations exceed
427 30 years, but approximately 24.3% of the AWSs still cover less than 5 years. For various reasons, most
428 of the time series in the dataset have gaps for one or all of the meteorological elements (Fig.9).

429 Fig.9 and Fig.S1-S4 show data availability of the daily air temperature, air pressure, wind speed and
430 relative humidity, respectively, calculated by more than 25% of the 3-hourly observations. Among the
431 267 AWSs, the air temperature measurement data have the best continuity and highest data integrity.
432 Approximately 30% of the stations have more than 15 years of daily temperature measurement data.
433 Furthermore, 237 stations have daily data integrity of more than 50%. In recent years, the improvement
434 of air pressure sensor technology has greatly enhanced the quality of air pressure measurement data. The
435 integrity of daily pressure data of 225 meteorological stations exceeds 50%, and approximately 28% of
436 stations have daily pressure data over a 15-year timespan. The wind sensor is obviously affected by
437 temperature, and the resulting data has the poorest continuity of data. Only approximately 28% of the
438 stations have the daily scalar wind speed and vector direction data with a timespan of more than 15 years.
439 There are 114 stations having daily scalar wind speed and vector wind direction data integrity of more
440 than 50%. For the 1980-2021 period, the lack of relative humidity data is the most serious, with 46 stations
441 having no relative humidity data all year round, and only 167 stations with daily data integrity of more
442 than 50%. Moreover, the data continuity is the lowest, with only 20% of stations measuring daily relative
443 humidity covering more than 15 years.



444
445
446

Fig. 9. Daily data availability of air temperature. Missing values have no colour, and 1-267 corresponds to the NO. in Table S1.

447 **6 Station documentation**

448 The entire dataset consists of four subdatasets, including three quality-controlled subdatasets and one
449 flagged subdataset of suspicious data in raw data, which are all provided in spreadsheet form. In quality-
450 controlled daily and monthly subdatasets, all "wt" columns are the proportion of observations entered into
451 the average value of the day or month. Number "1" indicates integrated continuous data without missing
452 data. In the flagged subdataset, "flag_*" marks the suspicious data of each variable detected in Section
453 3.2 quality control. Number "4" indicates that the observed value exceeds the three standard deviations
454 from the mean. A multiple of 100 represents the physically unrealistic 6-h rapid synoptic variability in
455 the parameters. The air temperature records in the austral summer months (December-January-February)
456 during the low-wind speed conditions (less than 2 m s^{-1}) are flagged with number "10000". Time is in 3-
457 hourly, daily and monthly formats, and the UTC time is used in the 3-hourly data files (UTC+8). At the
458 same time, we also provide the data integrity of 3-hourly, daily and monthly data of each variable.

459 The raw data we collected from different Antarctic AWS projects include four different data storage
460 formats: ASCII format (.dat), NetCDF format (.nc), TXT format (.txt) and Excel format (.xlsx). Five
461 meteorological elements are extracted and saved in comma separated values format (.csv format). CSV
462 format is selected due to its simple file structure and storage mode, basic security, and extensive support
463 in scientific applications, which is convenient for programming software (e.g., R) to process data in
464 batches. The file names are composed using the station's name and data type. A file name such as AGO
465 Site_3 h.csv can be read as station AGO Site, 3-hourly data, extension indicating CSV format data (.csv).
466 The data are arranged in columns of Year, Month, Day, Three-hourly observation time (UTC),
467 Temperature ($^{\circ}\text{C}$), Pressure (hPa), Wind Speed (m/s), Wind Direction ($^{\circ}$), Relative Humidity (%).

468 **7 Data and code availability**

469 The comprehensive AWS dataset is freely available as 3-hourly, daily, and monthly data separated for
470 each station at <https://amrddata.ssec.wisc.edu/dataset/antaws-dataset> (Wang et al., 2022). All codes for
471 the AWS data quality control are developed in the R environment, which are available from the
472 corresponding authors on a reasonable request.

473 **8 Conclusions**

474 We provide a comprehensive compilation of long-term measurements of the Antarctic AWSs. The dataset
475 includes the locations, instruments used, and measurements of five parameters i.e., air temperature, air
476 pressure, relative humidity, wind speed and wind direction, of 267 AWSs at 3-hourly, daily and monthly
477 resolutions, covering most areas of the Antarctic continent from 1980 to 2021. Relative to earlier studies,
478 our compilation presents better spatial coverage, although the spatial density is least over the East
479 Antarctic Plateau.

480 We adopt a comprehensive quality control process to carefully check the data to maximize the
481 reliability of the data. This results in the reduction in the temporal density of data in some AWSs. However,
482 the statistical results of 267 AWSs from 1980 to 2021 show that the integrity of the 3-hourly air

483 temperature and air pressure data from 192 stations exceeds 50%. Moreover, 159 stations have 3-hourly
484 relative humidity data integrity of more than 50%, which is the variable of lowest data integrity. There
485 are 92 stations with the integrity of the 3-hourly wind measurement data of less than 50%. This is easily
486 understood as among the five variables, wind speed and direction observations have highest uncertainties
487 caused by excessive speed, snow build-up, and so on.

488 The dataset can provide more accurate and effective input and verification data for the validation of
489 reanalyses, remote sensing products and regional climate models. At the same time, as done by Steig et
490 al. (2009), by combining the dataset with reanalysis data or remote sensing products, gridded data
491 products can be reconstructed, which can better display the temporal and spatial variation in the AIS
492 meteorological elements at different scales, and provide basic data for the studies of Antarctic mass
493 balance and climate changes. It is hoped that the dataset will facilitate glaciological, meteorological,
494 hydrological, or other studies over Antarctica.

495 The AWS network in the Antarctic is still incomplete and needs to be improved. In the future, it is
496 hopeful that more AWSs will be deployed on the East Antarctic Plateau as a priority, especially on the
497 summit of this region. However, it is highly challenging to install and maintain them in the extreme
498 environment of the East Antarctic Plateau. Moreover, ultrasonic sounders are systematically implemented,
499 to provide snow height data along with the meteorological data. Mechanically ventilated aspirated
500 radiation shields should be considered to reduce radiation bias, especially in summer when solar power
501 is available. In addition, the relative humidity supersaturated observation systems under extreme cold
502 conditions described by Genthon et al. (2017) and Genthon et al. (2022) can be widely applied. With the
503 continuous improvement of the AWS network and updating of AWS data, we will further refine the
504 dataset, adopt more rigorous quality control criteria, check the unrecognizable errors in the raw data, and
505 even provide quality marks for the dataset.

506 **Author contributions.**

507 YW contributed the idea of this work and constructed the AntAWS dataset. XZ prepared the figures
508 and tables based on the compiled data analysis. WN wrote the codes of data processing algorithm. MAL,
509 MD, CHR, PCJPS, PG and ERT provided part of AWS observations for constructing the dataset. MAL
510 and PG provided some necessary information of AWSs. ZZ and YS performed the primary data
511 collections. SH supervised this work. XZ and YW wrote the original draft, which was improved by all
512 other authors.

513 **Competing interests.**

514 All authors have declared that none of them have any conflicts of interest.

515 Acknowledgements

516 Funding this work was the National Natural Science Foundation of China (41971081, 41830644 and
517 42122047), the National Key Research and Development Program of China (2020YFA0608202), the
518 Strategic Priority Research Program of the Chinese Academy of Sciences (XDA19070103), the Project
519 for Outstanding Youth Innovation Team in the Universities of Shandong Province (2019KJH011) and the
520 Basic Research Fund of the Chinese Academy of Meteorological Sciences (2021Y021 and 2021Z006).
521 This work is also supported by funding to the University of Wisconsin-Madison and Madison Area
522 Technical College from the US National Science Foundation Office of Polar Programs (1924730,
523 1951720, and 1951603).

524 References

- 525 Allison, I., and Morrissy, J.V.: Automatic weather stations in Antarctica, *Australian Meteorological*
526 *Magazine*, 31, 71-76, 1983.
- 527 Allison, I., Wendler, G., and Radok, U.: Climatology of the East Antarctic ice sheet (100°E to 140°E)
528 derived from automatic weather stations, *Journal of Geophysical Research: Atmospheres*, 98, 8815-
529 8823, <https://doi.org/10.1029/93JD00104>, 1993.
- 530 Allison, I.: The surface climate of the interior of the Lambert Glacier basin: 5 years of automatic weather
531 station data, *Annals of Glaciology*, 27, 515-520, <https://doi:10.3189/1998AoG27-1-515-520>, 1998.
- 532 Amory, C.: Drifting-snow statistics from multiple-year autonomous measurements in Adélie Land, East
533 Antarctica, *The Cryosphere*, 14, 1713–1725, <https://doi.org/10.5194/tc-14-1713-2020>, 2020.
- 534 Aristidi, E., Agabi, K., Azouit, M., Azouit, M., Fossat, E., Vernin, J., Travouillon, T., Lawrence, J. S.,
535 Meyer, C., Storey, J. W. V., Halter, B., Roth W. L. and Walden, V.: An analysis of temperatures and
536 wind speeds above Dome C, Antarctica, *Astronomy & Astrophysics*, 430, 739-746,
537 <https://doi.org/10.1051/0004-6361:20041876>, 2005.
- 538 Bromwich, D. H., Nicolas, J. P., Monaghan, A. J., Lazzara, M. A., Keller, L. M., Weidner, G. A., and
539 Wilson, A. B.: Central West Antarctica among the most rapidly warming regions on Earth, *Nature*
540 *Geoscience*, 6, 139-145, <https://doi.org/10.1038/NGEO1671>, 2013.
- 541 Bromwich, D. H., Nicolas, J. P., Monaghan, A. J., Lazzara, M. A., Keller, L. M., Weidner, G. A., and
542 Wilson, A. B.: Correction: Corrigendum: Central West Antarctica among the most rapidly warming
543 regions on Earth, *Nature Geoscience*, 7, 76-76, <https://doi.org/10.1038/ngeo2016>, 2014.
- 544 Chen Liqi: Evidence of Arctic and Antarctic changes and their regulation of global climate change (future
545 findings since the fourth IPCC assessment report released, *Chinese journal of polar research*, 25, 1-6,
546 <https://doi:CNKI:SUN:JDYZ.0.2013-01-000>, 2013.
- 547 Convey, P., Coulson, S. J., Worland, M. R., and Sjöblom, A.: The importance of understanding annual
548 and shorter-term temperature patterns and variation in the surface levels of polar soils for terrestrial
549 biota, *Polar Biology*, 41, 1587-1605, <https://doi.org/10.1007/s00300-018-2299-0>, 2018.
- 550 Donat-Magnin, M., Jourdain, N. C., Gallée, H., Amory, C., Kittel, C., Fettweis, X., Wille, J. D., Favier,
551 V., Drira, A., and Agosta, C.: Interannual variability of summer surface mass balance and surface

552 melting in the Amundsen sector, West Antarctica, *The Cryosphere*, 14, 229–249,
553 <https://doi.org/10.5194/tc-14-229-2020>, 2020.

554 Gallée, H., and Gorodetskaya, I. V.: Validation of a limited area model over Dome C, Antarctic Plateau,
555 during winter, *Climate dynamics*, 34, 61–72, <https://doi.org/10.1007/s00382-008-0499-y>, 2010.

556 Genthon, C., Six, D., Favier, V., Lazzara, M., and Keller, L.: Atmospheric temperature measurement
557 biases on the Antarctic plateau, *Journal of Atmospheric and Oceanic Technology*, 28, 1598–1605,
558 <https://doi.org/10.1175/JTECH-D-11-00095.1>, 2011.

559 Genthon, C., Six, D., Gallée, H., Grigioni, P., and Pellegrini, A.: Two years of atmospheric boundary
560 layer observations on a 45-m tower at Dome C on the Antarctic plateau, *Journal of Geophysical*
561 *Research: Atmospheres*, 118, 3218–3232, <https://doi.org/10.1002/jgrd.50128>, 2013.

562 Genthon, C., Piard, L., Vignon, E., Madeleine, J.-B., Casado, M., and Gallée, H.: Atmospheric moisture
563 supersaturation in the near-surface atmosphere at Dome C, Antarctic Plateau, *Atmos. Chem. Phys.*, 17,
564 691–704, <https://doi.org/10.5194/acp-17-691-2017>, 2017.

565 Genthon, C., Veron, D., Vignon, E., Six, D., Dufresne, J.-L., Madeleine, J.-B., Sultan, E., and Forget, F.:
566 10 years of temperature and wind observation on a 45 m tower at Dome C, East Antarctic plateau, *Earth*
567 *Syst. Sci. Data*, 13, 5731–5746, <https://doi.org/10.5194/essd-13-5731-2021>, 2021.

568 Genthon, C., Veron, D. E., Vignon, E., Madeleine, J.-B., and Piard, L.: Water vapor in cold and clean
569 atmosphere: a 3-year data set in the boundary layer of Dome C, East Antarctic Plateau, *Earth Syst. Sci.*
570 *Data*, 14, 1571–1580, <https://doi.org/10.5194/essd-14-1571-2022>, 2022.

571 Goff, J. A. and Gratch, S.: Thermodynamic properties of moist air, *Trans. ASHVE*, 51, 125, 1945.

572 Gregory, J. M., and Huybrechts, P.: Ice-sheet contributions to future sea-level change, *Philosophical*
573 *Transactions of the Royal Society A: Mathematical, Physical and Engineering Sciences*, 364, 1709–
574 1732, <https://doi.org/10.1098/rsta.2006.1796>, 2006.

575 Giovinetto, M. B., Waters, N. M., and Bentley, C. R.: Dependence of Antarctic surface mass balance on
576 temperature, elevation, and distance to open ocean, *Journal of Geophysical Research: Atmospheres*,
577 95, 3517–3531, <https://doi.org/10.1029/JD095iD04p03517>, 1990.

578 Herbei, R., Rytel, A. L., Lyons, W. B., McKnight, D. M., Jaros, C., Gooseff, M. N., and Priscu, J. C.:
579 Hydrological Controls on Ecosystem Dynamics in Lake Fryxell, Antarctica, *PloS one*, 11,
580 e01590382016, <https://doi.org/10.1371/journal.pone.0159038>, 2016.

581 Huai, B., Wang, Y., Ding, M., Zhang, J., and Dong, X.: An assessment of recent global atmospheric
582 reanalyses for Antarctic near surface air temperature, *Atmospheric Research*, 226, 181–191,
583 <https://doi.org/10.1016/j.atmosres.2019.04.029>, 2019.

584 Intergovernmental Panel on Climate Change.: IPCC special report on the ocean and cryosphere in a
585 changing climate, <https://archive.ipcc.ch/srocc/>, 2019.

586 Jacka, T. H.: A data bank of mean monthly and annual surface temperatures for Antarctica, the Southern
587 Ocean and South Pacific Ocean, Antarctic Division, Department of Science and Technology, 22, 98pp,
588 1984.

589 Jones, P. D., and Limbert, D W. S.: A data bank of Antarctic surface temperature and pressure data, East
590 Anglia Univ. (UK). Climatic Research Unit; British Antarctic Survey, Cambridge, DOE/ER/60397-H2,
591 52pp, 1987.

592 Jones, R., Renfrew, I., Orr, A., Webber, B., Holland, D., and Lazzara, M.: Evaluation of four global
593 reanalysis products using in situ observations in the Amundsen Sea Embayment, Antarctica, *Journal of*
594 *Geophysical Research: Atmospheres*, <https://doi.org/10.1002/2015JD024680>, 121, 6240–6257, 2016.

595 Kennicutt, M. C. II, Bromwich, D., Liggett, D., Njåstad, B., Peck, L., Rintoul, S. R., Ritz, C., Siegert, M.
596 J., Aitken, A., Brooks, C. M., Cassano, J., Chaturvedi, S., Chen, D., Dodds, K., Golledge, N. R., Bohec,
597 C. L., Leppe, M., Murray, A., Nath, P. C., Raphael, M. N., Rogan-Finnemore, M., Schroeder, D. M.,
598 Talley, L., Travouillon, T., Vaughan, D. G., Wang, L., Weatherwax, A. T., Yang, H., Chown, S. L.:
599 Sustained Antarctic research: a 21st century imperative, *One Earth*, 1, 95–113,
600 <https://doi.org/10.1016/j.oneear.2019.08.014>, 2019.

601 Kittel, C.: Present and future sensitivity of the Antarctic surface mass balance to oceanic and atmospheric
602 forcings: insights with the regional climate model MAR, PhD thesis, University of Liège, Liège,
603 <http://hdl.handle.net/2268/258491> (last access: 28 May 2022), 2021

604 Kittel, C., Amory, C., Agosta, C., Jourdain, N. C., Hofer, S., Delhasse, A., Doutreloup, S., Huot, P.-V.,
605 Lang, C., Fichet, T., and Fettweis, X.: Diverging future surface mass balance between the Antarctic
606 ice shelves and grounded ice sheet, *The Cryosphere*, 15, 1215–1236, [https://doi.org/10.5194/tc-15-](https://doi.org/10.5194/tc-15-1215-2021)
607 [1215-2021](https://doi.org/10.5194/tc-15-1215-2021), 2021.

608 Knuth, S. L., Tripoli, G. J., Thom, J. E., Weidner, G. A., The influence of blowing snow and precipitation
609 on snow depth change across the Ross Ice Shelf and Ross Sea regions of Antarctica, *Journal of Applied*
610 *Meteorology and Climatology*, 49, 1306-1321, <https://doi.org/10.1175/2010JAMC2245.1>, 2010.

611 Lazzara, M. A., Keller, L. M., Markle, T., and Gallagher, J.: Fifty-year Amundsen-Scott South Pole
612 station surface climatology, *Atmospheric Research*, 118, 240-259,
613 <https://doi.org/10.1016/j.atmosres.2012.06.027>, 2012.

614 Lazzara, M. A., Weidner, G. A., Keller, L. M., Thom, J. E., and Cassano, J. J.: Antarctic automatic
615 weather station program: 30 years of polar observation, *Bulletin of the American Meteorological*
616 *Society*, 93: 1519-1537, <https://doi.org/10.1175/BAMS-D-11-00015.1>, 2012.

617 Lazzara, M. A., Welhouse, L. J., Thom, J. E., Cassano, J. J., DuVivier, A. K., Weidner, G. A., Keller, L.
618 M., and Kalnajs, L.: Automatic Weather Station (AWS) Program operated by the University of
619 Wisconsin-Madison during the 2011-2012 field season, *Antarctic Record*, 57, 125-135,
620 <http://doi.org/10.15094/00009683>, 2013.

621 Ma, Y., Bian, L., Xiao, C., Allison, I.: Correction of snow accumulation impacted on air temperature from
622 automatic weather station on the Antarctic Ice Sheet. *Advance in Polar Science*, 20: 299-309,
623 <http://ir.casnw.net/handle/362004/7877>, 2008.

624 Ma, Y., and Bian, L.: A Surface Climatological Validation of ERA-interim Reanalysis and NCEP FNL
625 Analysis over East Antarctic, *Chinese Journal of Polar Research*, 26, 469-480.,
626 <https://doi.org/10.13679/j.jdyj.2014.4.469>, 2014

627 Masson-Delmotte, V., Zhai, P., Pirani, A., Connors, S. L., Péan, C., Berger, S., Caud, N., Chen, Y.,
628 Goldfarb, L., Gomis, M.I., Huang, M., Leitzell, K., Lonnoy, E., Matthews, J. B. R., Maycock, T. K.,
629 Waterfield, T., Yelekçi, O., Yu, R., and Zhou, B. (eds.): IPCC, 2021: Climate Change 2021: The
630 Physical Science Basis. Contribution of Working Group I to the Sixth Assessment Report of the
631 Intergovernmental Panel on Climate Change, Cambridge University Press. In Press.
632 <https://www.ipcc.ch/report/ar6/wg1/>.

633 Mottram, R., Hansen, N., Kittel, C., van Wessem, J. M., Agosta, C., Amory, C., Boberg, F., van de Berg,
634 W. J., Fettweis, X., Gossart, A., van Lipzig, N. P. M., van Meijgaard, E., Orr, A., Phillips, T., Webster,
635 S., Simonsen, S. B., and Souverijns, N.: What is the surface mass balance of Antarctica? An
636 intercomparison of regional climate model estimates, *The Cryosphere*, 15, 3751–3784,
637 <https://doi.org/10.5194/tc-15-3751-2021>, 2021.

638 Reijmer, C. H., and Oerlemans, J.: Temporal and spatial variability of the surface energy balance in
639 Dronning Maud Land, East Antarctica, *Journal of Geophysical Research: Atmospheres*, 107, 4759,
640 <https://doi.org/10.1029/2000JD000110>, 2002.

641 Renfrew, I. A., and Anderson, P. S.: The surface climatology of an ordinary katabatic wind regime in
642 Coats Land, Antarctica, *Tellus A: Dynamic Meteorology and Oceanography*, 54: 463-484,
643 <https://doi.org/10.3402/tellusa.v54i5.12162>, 2002.

644 Reusch, D. B., Alley, R. B.: A 15-year West Antarctic climatology from six automatic weather station
645 temperature and pressure records, *Journal of Geophysical Research: Atmospheres*, 109, D04103,
646 <https://doi.org/10.1029/2003JD004178>, 2004.

647 Rodrigo, J. S., Buchlin, J-M., van Beeck J., Lenaerts, J. T. M., van den Broeke, M. R.: Evaluation of the
648 antarctic surface wind climate from ERA reanalyses and RACMO2/ANT simulations based on
649 automatic weather stations, *Climate Dynamics*, 40, 353–376, <https://doi.org/10.1007/s00382-012-1396-y>, 2013.

650 Rignot, E., Mouginot, J., Scheuchl, B., and Morlighem, M.: Four decades of Antarctic Ice Sheet mass
651 balance from 1979–2017, *PNAS*, 116, 1095-1103, <https://doi.org/10.1073/pnas.1812883116>, 2019.

652 Seefeldt, M. W., Cassano, J. J., Parish, T. R.: Dominant regimes of the Ross Ice Shelf surface wind field
653 during austral autumn 2005, *Journal of applied meteorology and climatology*, 46, 1933-1955,
654 <https://doi.org/10.1175/2007JAMC1442.1>, 2007.

655 Shuman, C. A., Stearns, C. R.: Decadal-length composite inland West Antarctic temperature records.
656 *Journal of Climate*, 14, 1977-1988, [https://doi.org/10.1175/1520-0442\(2001\)014<1977:DLCIWA>2.0.CO;2](https://doi.org/10.1175/1520-0442(2001)014<1977:DLCIWA>2.0.CO;2), 2001.

657 Smeets, P. C., Kuipers Munneke, P., Van As, D., van den Broeke, M. R., Boot, W., Oerlemans, H., Snellen,
658 H., Reijmer, C.H., and van de Wal, R. S.: The K-transect in west Greenland: Automatic weather station
659 data (1993-2016), *Arctic, Antarctic, and Alpine Research*, 50, S100002,
660 <https://doi.org/10.1080/15230430.2017.1420954>, 2018.

661 Stearns, C. R., Keller, L. M., Weidner, G. A., and Sievers, M.: Monthly mean climatic data for Antarctic
662 automatic weather stations, *Antarctic meteorology and climatology: studies based on automatic
663 weather stations*, 61: 1-21, <https://doi.org/10.1029/AR061p0001>, 1993.

664 Stearns, C. R., Wendler, G.: Research results from Antarctic automatic weather stations, *Reviews of
665 Geophysics*, 26: 45-61, <https://doi.org/10.1029/RG026i001p00045>, 1988.

666 Steig, E. J., Schneider, D. P., Rutherford, S. D., Mann, M. E., Comiso, J. C., and Shindell, D. T.: Warming
667 of the Antarctic ice-sheet surface since the 1957 International Geophysical Year, *Nature*, 457, 459-462,
668 <https://doi.org/10.1038/nature07669>, 2009.

669 Summerhayes, C. P.: International collaboration in Antarctica: The International Polar Years, the
670 International Geophysical Year, and the Scientific Committee on Antarctic Research, *Polar
671 Record*, 44, 321–334, <https://doi.org/10.1017/S0032247408007468>, 2008.

- 674 Tastula, E. M., Vihma, T., and Andreas, E. L.: Evaluation of Polar WRF from Modeling the Atmospheric
675 Boundary Layer over Antarctic Sea Ice in Autumn and Winter, *Monthly weather review*, 140, 3919-
676 3935, <https://doi.org/10.1175/MWR-D-12-00016.1>, 2012.
- 677 Turner, J., Colwell, S. R., Marshall, G. J., Lachlan-Cope, T. A., Carleton, A. M., Jones, P. D., Lagun, V.,
678 Reid, P. A., and Iagovkina, S.: The SCAR READER project: Toward a high-quality database of mean
679 Antarctic meteorological observations, *Journal of Climate*, 17, 2890-2898,
680 [https://doi.org/10.1175/1520-0442\(2004\)017<2890:TSRPTA>2.0.CO;2](https://doi.org/10.1175/1520-0442(2004)017<2890:TSRPTA>2.0.CO;2), 2004.
- 681 Van den Broeke, M. R., Van Lipzig, N. P. M., and Van Meijgaard, E.: Momentum budget of the East
682 Antarctic atmospheric boundary layer: Results of a regional climate model, *Journal of the Atmospheric
683 Sciences*, 59, 3117-3129, [https://doi.org/10.1175/1520-0469\(2002\)059<3117:MBOTEA>2.0.CO;2](https://doi.org/10.1175/1520-0469(2002)059<3117:MBOTEA>2.0.CO;2),
684 2002.
- 685 Van den Broeke, M. R., and Van Lipzig, N. P. M.: Factors controlling the near-surface wind field in
686 Antarctica, *Monthly Weather Review*, 131, 733-743, [https://doi.org/10.1175/1520-0493\(2003\)131<0733:FCTNSW>2.0.CO;2](https://doi.org/10.1175/1520-0493(2003)131<0733:FCTNSW>2.0.CO;2), 2003.
- 687 Van Wessem, J. M., Reijmer, C. H., Lenaerts, J. T. M., van de Berg, W. J., van den Broeke M. R., van
688 Meijgaard, E. Updated cloud physics in a regional atmospheric climate model improves the modelled
689 surface energy balance of Antarctica, *The Cryosphere*, 8, 125–135, <https://doi.org/10.5194/tc-8-125-2014>, 2014.
- 690 Wang, Y., Ding, M., Reijmer, C. H., Smeets, P. J. P., Hou, S., Xiao, C.: The AntSMB dataset: a
691 comprehensive compilation of surface mass balance field observations over the Antarctic Ice Sheet.
692 *Earth System Science Data*, 13, 3057-3074, <https://doi.org/10.5194/essd-13-3057-2021>, 2021.
- 693 Wang, Y., Wang, M., and Zhao, J.: A comparison of MODIS LST retrievals with in situ observations
694 from AWS over the Lambert Glacier Basin, East Antarctica, *International Journal of Geosciences*, 4,
695 611-617, <https://doi.org/10.4236/ijg.2013.43056>, 2013.
- 696 Wang, Y., Zhang, X., Ning, W., Lazzara, M. A., Ding, M., Reijmer C., Smeets P., Grigioni, P., Thomas,
697 E.R., Zhai Z., Sun Y., Hou, S.: AntAWS Dataset: A compilation of Antarctic automatic weather station
698 observations. Version 1.0. AMRDC Data Repository, <https://doi.org/10.48567/key7-ch19>, 2022.
- 699 Wild, M., Calanca, P., Scherrer, S. C., and Ohmura, A.: Effects of polar ice sheets on global sea level in
700 high-resolution greenhouse scenarios, *Journal of Geophysical Research: Atmospheres*, 108, 4165,
701 <https://doi.org/10.1029/2002JD002451>, 2003.
- 702 Wille, J.D., Favier, V., Jourdain, N.C. et al. Intense atmospheric rivers can weaken ice shelf stability at
703 the Antarctic Peninsula. *Commun Earth Environ* 3, 90. <https://doi.org/10.1038/s43247-022-00422-9>.
704 2022
- 705 World Meteorological Organization: Guide to Instruments and Methods of Observation Volume 1–
706 Measurement of Meteorological Variables, Geneva, Switzerland, 8, 2018.